



Supplement of

Formation of nighttime sulfuric acid from the ozonolysis of alkenes in Beijing

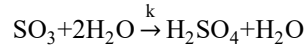
Yishuo Guo et al.

Correspondence to: Chao Yan (chao.yan@helsinki.fi)

The copyright of individual parts of the supplement might differ from the article licence.

S1. Conversion of SO₃ to SA

The conversion of SO₃ to SA is based on the following reaction:



The production rate of SA from SO₃ is:

$$P_{[\text{SA}]} = k[\text{SO}_3][\text{H}_2\text{O}]^2$$

where $k = 3.9 \times 10^{-41} \exp(6830.6/T) \text{ cm}^{-6} \text{ s}^{-1}$ (Jayne et al., 1997). During the measurement period, nighttime median concentration of H₂O was $4.97 \times 10^{16} \text{ cm}^3$, and nighttime median temperature was 276.6 K, then:

$$k[\text{H}_2\text{O}]^2 = [3.9 \times 10^{-41} \exp(6830.9/276.6) \text{ cm}^{-6} \text{ s}^{-1}] \times (4.97 \times 10^{16} \text{ cm}^3)^2 = 4.88 \times 10^3 \text{ s}^{-1}$$

The lifetime of SO₃ based on reaction with H₂O is:

$$\tau_{\text{SO}_3} = \frac{1}{k[\text{H}_2\text{O}]^2} = \frac{1}{4.88 \times 10^3 \text{ s}^{-1}} = 2.05 \times 10^{-4} \text{ s}$$

The lifetime of SO₃ is so short under typical atmospheric conditions, which means that the reaction between SO₃ and H₂O is so fast that all SO₃ will be instantaneously converted to SA. In this case, the oxidation of SO₂ is the rate-limiting step in the formation of SA.

S2. Pseudo-steady-state (PSS) assumption of SA

The net concentration change of gaseous SA is determined by both the source and loss terms, as shown in the following equation:

$$\frac{d[\text{SA}]}{dt} = k_{\text{app}}[\text{Alkene}][\text{O}_3][\text{SO}_2] - [\text{SA}]CS - \beta[\text{SA}]^2$$

where the loss rate and production rate of SA are $L_{\text{SA}} = [\text{SA}]CS + \beta[\text{SA}]^2$ and $P_{\text{SA}} = L_{\text{SA}} + d[\text{SA}]/dt$ respectively. We can compare the magnitude of the net concentration change to the overall loss rate. During nighttime (20:00-04:00) from 18th January to 16th March 2019, the median net concentration change of SA is about $181.60 \text{ cm}^{-3} \text{ s}^{-1}$ and the overall SA loss rate at the median SA concentration ($7.52 \times 10^5 \text{ cm}^{-3}$) is $1.61 \times 10^4 \text{ cm}^{-3} \text{ s}^{-1}$. As the loss rate (and source rate) is much faster than the net concentration change, the pseudo-steady state (PSS) assumption is valid for SA. Besides, the resolution of the SA data is 5 minutes, and the concentration, net concentration change, loss rate and production rate of SA are listed in Table S4.

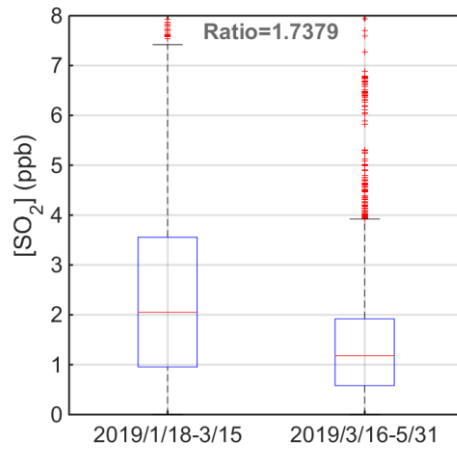
S3. Division of pollution level by visibility

Pollution level is kind of an ambiguous concept, and one may judge it by PM_{2.5}, while another may judge it by visibility or NO_x. Therefore, we did some efforts to determine the final parameter used to represent pollution level. Fig. S3 shows the correlation of PM_{2.5}, CS, RH with visibility. It can be seen that with the increase of visibility, PM_{2.5} decreases monotonically, and RH and CS also have a declining trend. Hence, visibility is a good candidate to represent pollution level. Besides, in the visibility range of 12.0 km to 19.0 km, with the increase of visibility, PM_{2.5} and RH do not vary too much, with CS slightly declining as well, which also implies that visibility is more sensitive than PM_{2.5}, RH and CS. Thus, visibility indeed can be used to judge the pollution level for this specific time period of this study.

It also can be found out that the correlation between PM_{2.5} and visibility can be further divided into the following 3 groups:
a. visibility < 4.0 km (heavy polluted conditions): visibility and PM_{2.5} have a very good negative linear correlation with R₁ (correlation coefficient) = -1.00, and the decrease rate of visibility is rather fast with the slope of $k_1 = -0.0339 \mu\text{g}/\text{m}^4$;
b. 4.0 km ≤ visibility < 12.0 km (mildly polluted conditions): visibility and PM_{2.5} also have a negative linear correlation with R₂ = -0.97, but the decrease rate of visibility with PM_{2.5} reduces to $k_2 = -0.0084 \mu\text{g}/\text{m}^4$;
c. visibility ≥ 12.0 km (clean conditions): PM_{2.5} stays constant with varying visibility values, which means that when PM_{2.5} is smaller than $40 \mu\text{g}/\text{m}^3$ during heating

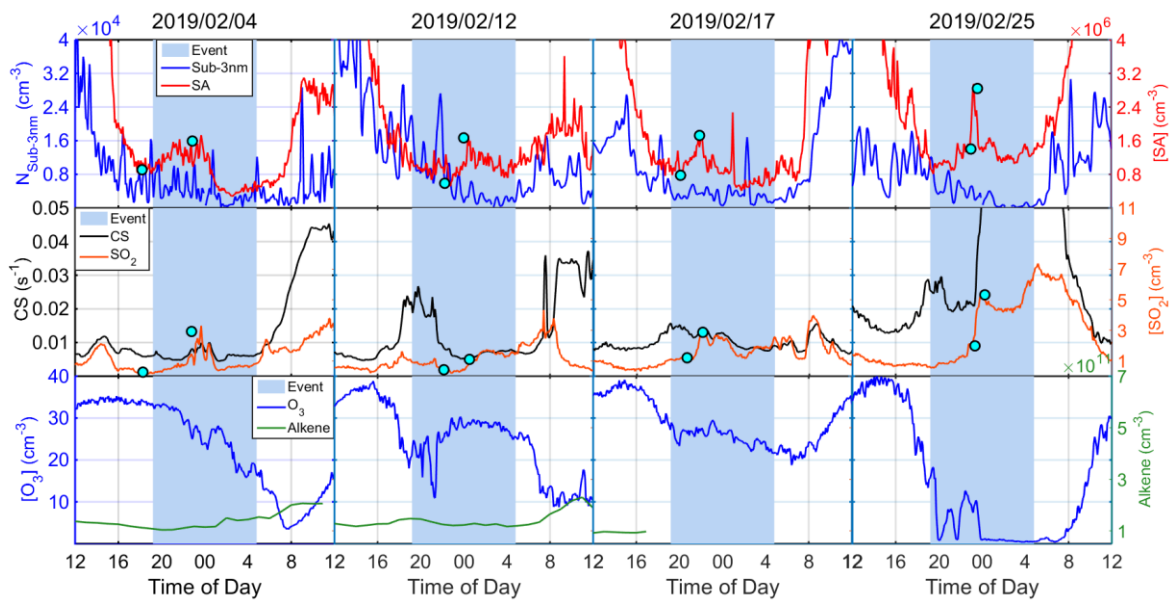
supply winter period, visibility will be more likely influenced by other factors. In total, data points under the clean conditions mentioned above take up 47.91% of all data points.

Figures



45

Fig. S1 Boxplot for SO_2 mixing ratio during nighttime (20:00-04:00 next day) in winter-heating-supply period (from 18th January to 15th March 2019) and non-heating-supply period (from 16th March 2019 to 31st May 2019). The middle line in the box is the median, the bottom and the top are the 25 and 75 percentiles, the whisker ranges cover the $\pm 2.7\sigma$ of data in each group, and the red points are the outliers. The dark gray value on the top is the ratio between median SO_2 values of two periods.



50

Fig. S2 Daily time-series of different parameters on nighttime SA event days when SA cases occurred under SO_2 increase condition. The first row: $N_{\text{Sub-3nm}}$ and SA concentration, the second row: CS and SO_2 concentration, and the third row: concentration of O_3 and alkenes. The increase starting points and maximum value points of SA concentration as well as the corresponding SO_2 concentration at the same moments are marked by cyan dots.

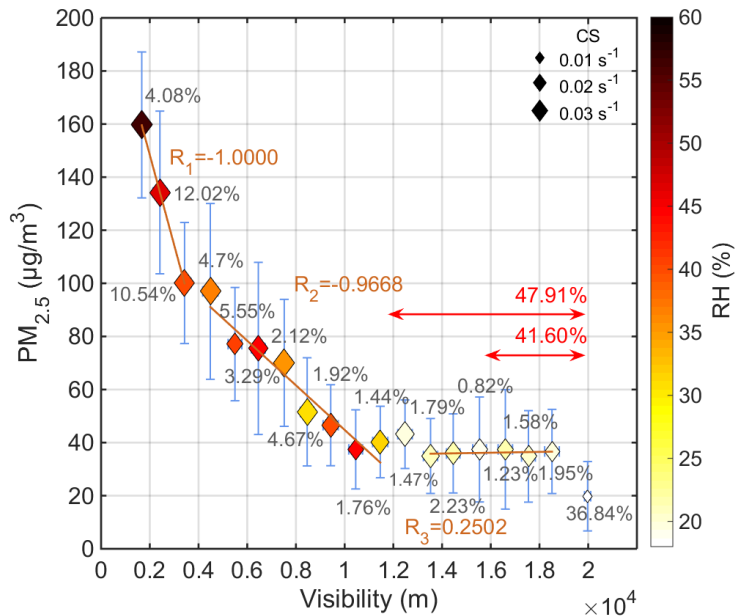


Fig. S3 Correlation between $PM_{2.5}$ and visibility during nighttime (20:00-04:00 next day) from 18th January to 15th March 2019. The size is proportional to CS and the color is based on RH. Note that the data points are based on data averaged and binned into different visibility ranges instead of the original, high time resolution ones. The error bars are the standard deviation of all data points in each bin.

55

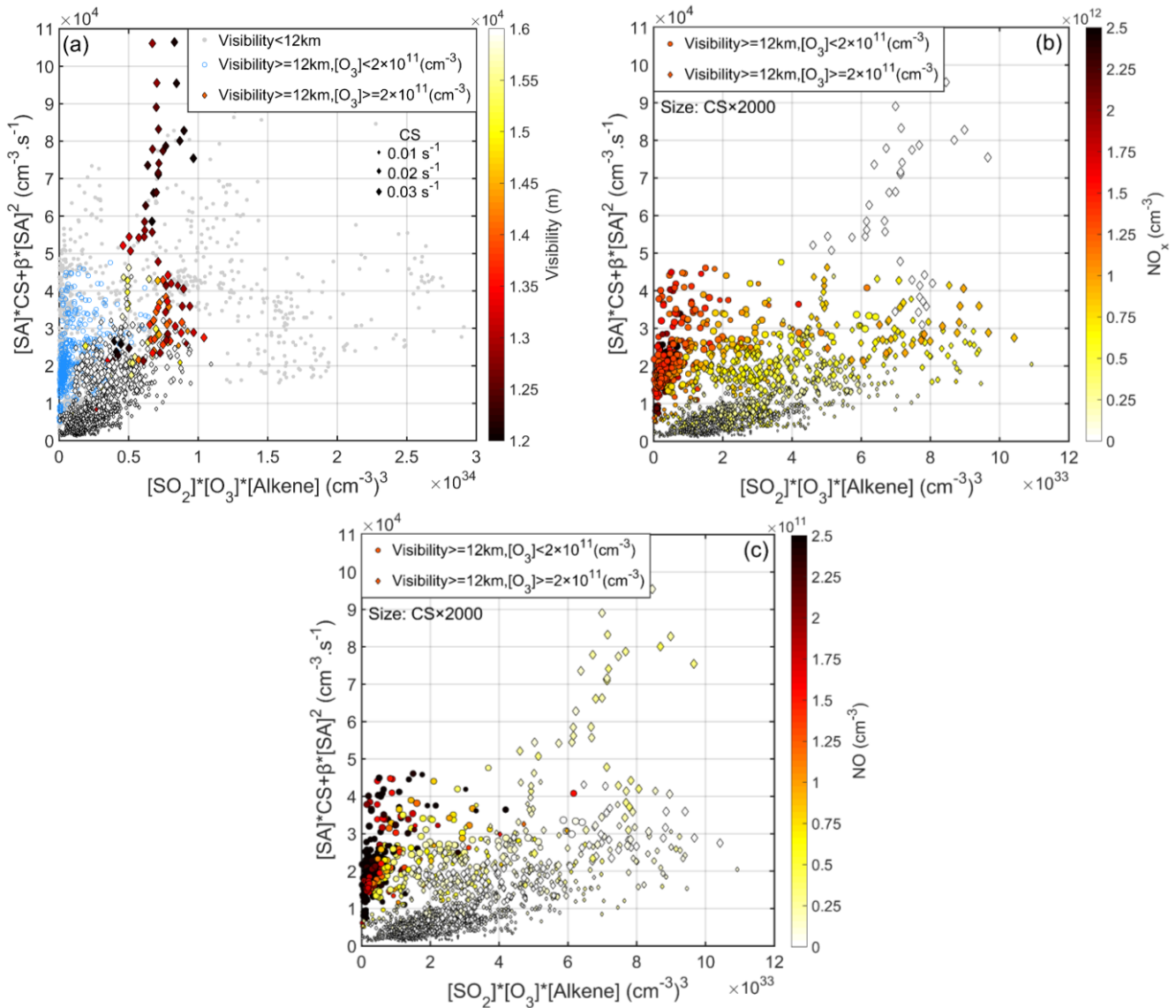


Fig. S4 Nighttime correlation between the source term ($[SO_2][O_3][Alkene]$) and sink term ($[SA]CS+\beta[SA]^2$) of SA under PSS assumption during nighttime (20:00-04:00 next day) from 18th January to 15th March 2019 for (a) with all data points divided by O_3 concentration and visibility, (b) and (c) with data points having visibility larger than 12.0 km divided by $[O_3]$ and colored by NO_x and NO respectively.

60

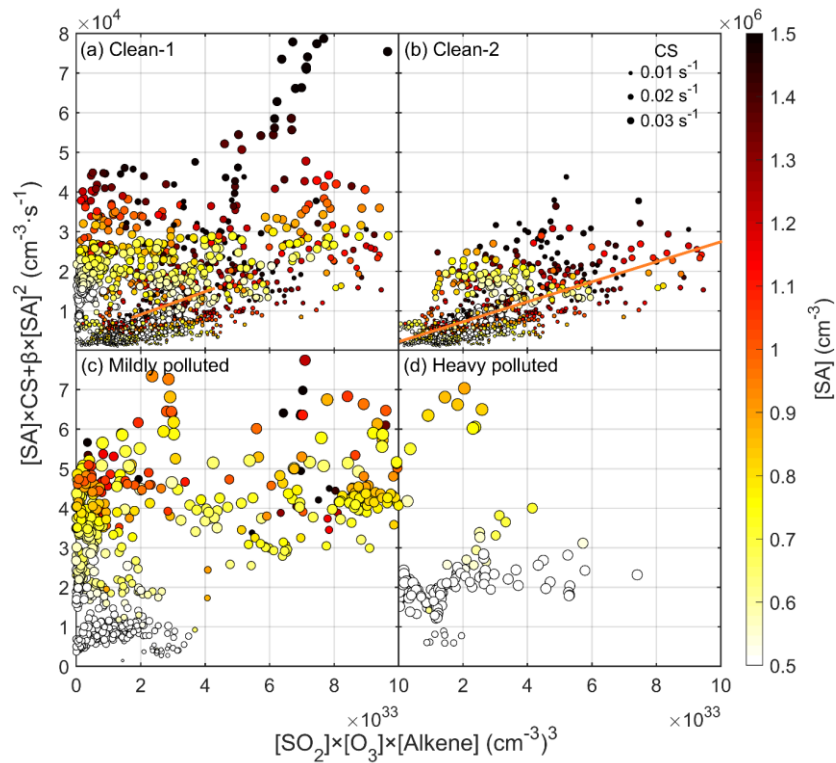
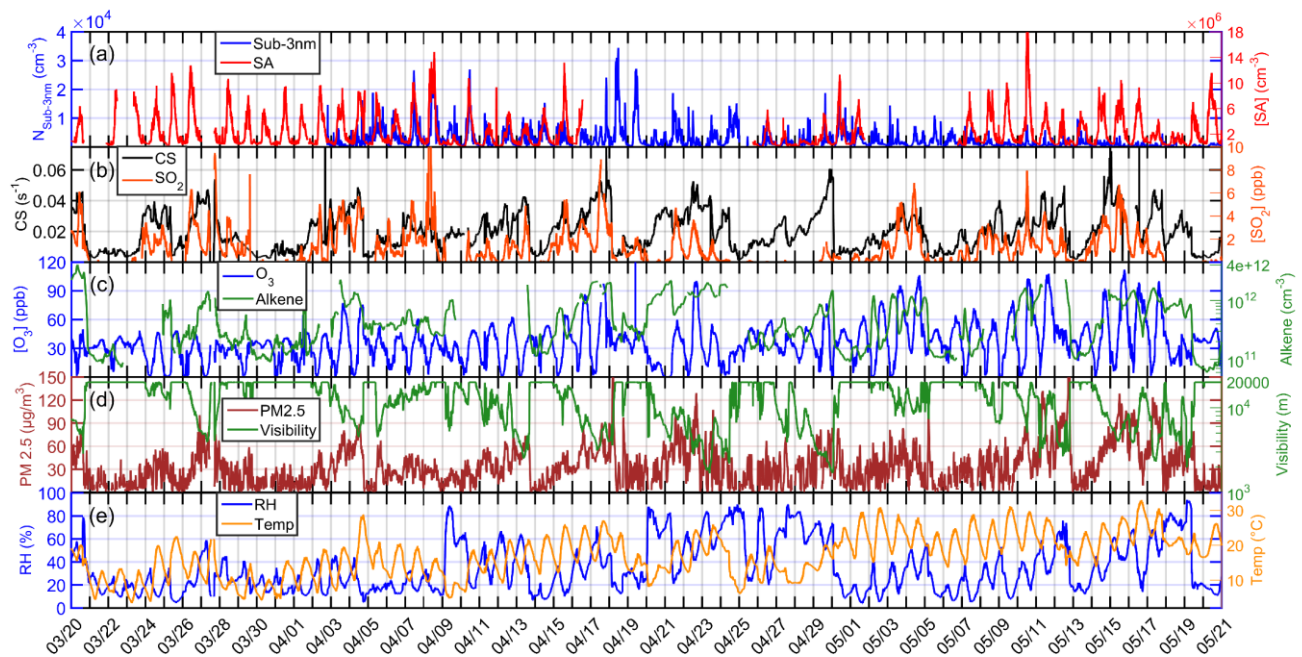
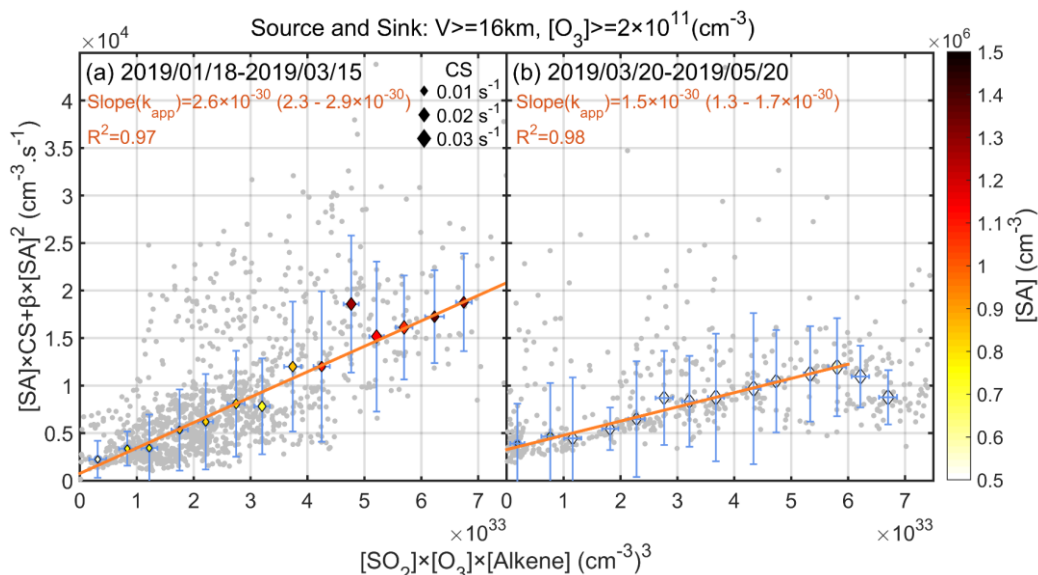


Fig. S5 Nighttime correlation between the source term ($[\text{SO}_2][\text{O}_3][\text{Alkene}]$) and sink term ($[\text{SA}]\text{CS} + \beta[\text{SA}]^2$) of SA under PSS assumption for (a) Clean-1 condition, (b) Clean-2 condition, (c) mildly polluted condition and (d) heavy polluted condition.

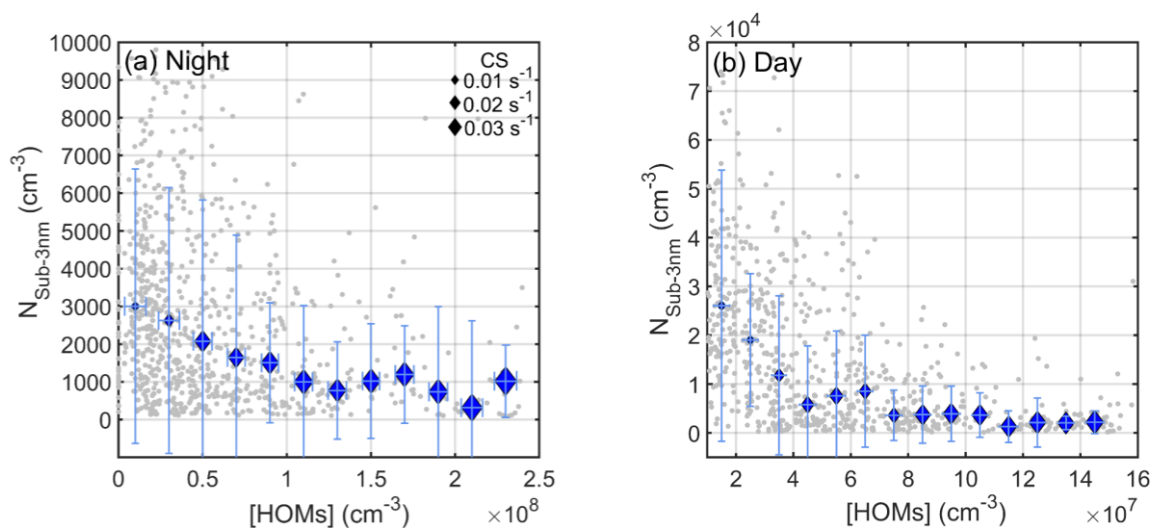


65 Fig. S6 Time variation of different parameters measured from 20th March to 20th May 2019 for (a) SA concentration and $N_{\text{Sub-3nm}}$, (b) CS and SO_2 concentration, (c) concentration of O_3 and alkenes, (d) $\text{PM}_{2.5}$ and visibility, and (e) relative humidity (RH) and temperature.



70

Fig. S7 Nighttime correlation between the source term ($[\text{SO}_2][\text{O}_3][\text{Alkene}]$) and sink term ($[\text{SA}]\text{CS} + \beta[\text{SA}]^2$) under clean conditions for (a) from 18th January to 15th March 2019 and (b) from 20th March to 20th May 2019. The gray dots are original, high time resolution data, and the diamond points are based on data median averaged and binned to different source ranges instead of the original, high time resolution data. The error bars are the standard deviation of all data points in each bin.



75

Fig. S8 Correlation between $N_{\text{Sub-3nm}}$ and number concentration of HOMs for (a) during nighttime (20:00-04:00 next day) and (b) during daytime (09:00-16:00) from 18th January to 15th March 2019. Grey dots are original data, and diamonds are binned ones. The size of the binned data is proportional to CS and blue lines are standard deviation of each binned data.

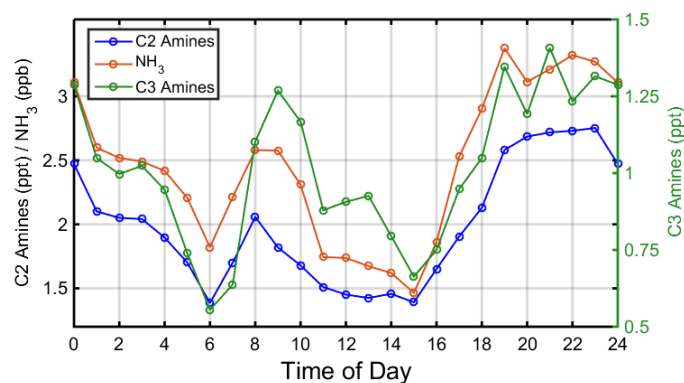
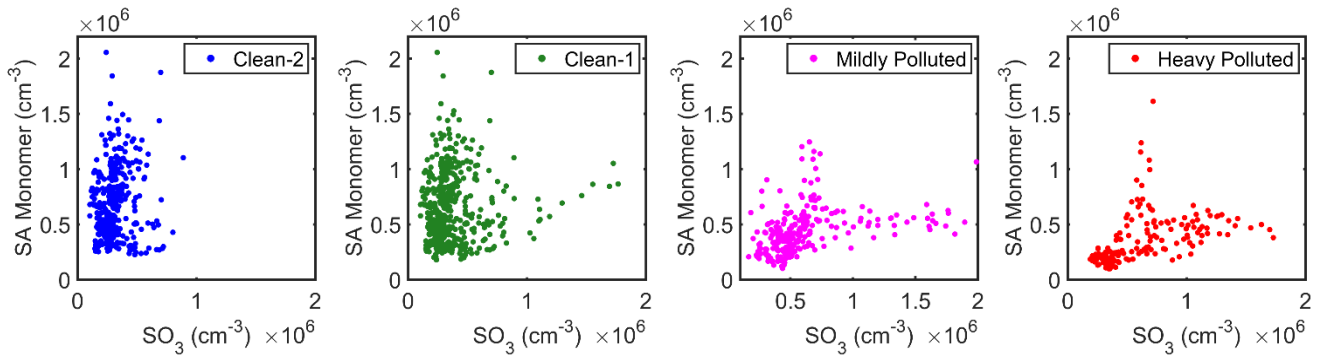


Fig. S9 Median diurnal variation of NH_3 , C2 amines and C3 amines from 10th December, 2018 to 6th January, 2019.



80

Fig. S10 Correlation between sulfuric acid monomer and SO_2 measured by CI-APi-TOF during nighttime (20:00 – 04:00 next day) from 18th January to 15th March 2019 for (a) Clean-2 condition with visibility larger than 16.0 km and O_3 concentration higher than $2.0 \times 10^{11} \text{ cm}^{-3}$ (~ 7 ppb), (b) Clean-1 condition with visibility larger than 12.0 km, (c) mildly polluted condition with visibility in the range of 4.0 - 12.0 km, and (d) heavy polluted condition with visibility smaller than 4.0 km.

Table S1 Dates of Nighttime SA event and non-event days.

Nighttime SA Event Day	Nighttime SA Non-event Day
2019.01.20	2019.01.24
2019.01.21	2019.01.30
2019.01.22	2019.02.03
2019.01.23	2019.02.06
2019.01.25	2019.02.08
2019.01.28	2019.02.11
2019.02.01	2019.02.13
2019.02.04	2019.02.21
2019.02.12	2019.02.22
2019.02.15	2019.02.27
2019.02.17	2019.03.04
2019.02.20	2019.03.06
2019.02.25	2019.03.07
2019.02.26	2019.03.09
2019.02.28	2019.03.10
2019.03.12	2019.03.11
2019.03.14	
2019.03.15	

Table S2 Features of Nighttime SA Event Cases on 18 Event Nights.

Date	Number of Nighttime SA Case	CS Decrease Case	SO ₂ Increase Case	Other Cases
2019.01.20	1			1
2019.01.21	1	1		
2019.01.22	1	1		
2019.01.23	1	1		
2019.01.25	1	1		
2019.01.28	1			1
2019.02.01	1			1
2019.02.04	1		1	
2019.02.12	2	1	1	
2019.02.15	1	1		
2019.02.17	1		1	
2019.02.20	1		No CS data	
2019.02.25	1			
2019.02.26	2	2		
2019.02.28	1		No CS data	
2019.03.12	1		No CS data	
2019.03.14	1		No CS data	
2019.03.15	1		No CS data	
Total	15 with CS data (20 in total)	8 (53.33%*)	4 (26.67%*)	3 (20.00%*)

* There are 5 days when CS data is not available and the statistical percentages in the brackets are based on the CS available cases.

Table S3 Fitted value, 95% confidence bounds and uncertainty of k_{app} and R^2 for Clean-1 and Clean-2 condition.

Condition	k_{app} (cm ⁶ s ⁻¹)	95% Confidence Bounds (cm ⁶ s ⁻¹)	Uncertainty (%)	R^2
Clean-1	2.7×10^{-30}	$2.1 \times 10^{-30} - 3.2 \times 10^{-30}$	20.2	0.97
Clean-2	2.6×10^{-30}	$2.3 \times 10^{-30} - 2.9 \times 10^{-30}$	11.3	0.97

Table S4 Concentration, net concentration change, loss rate and production rate of SA during nighttime (20:00-04:00 next day) from 18th January to 15th March 2019.

	[SA] (cm ⁻³)	d[SA]/dt (cm ⁻³ s ⁻¹)	L _{SA} (cm ⁻³ s ⁻¹)	P _{SA} (cm ⁻³ s ⁻¹)
Median	7.52×10^5	181.60	1.61×10^4	1.60×10^4
25 percentile	5.19×10^5	78.37	4.83×10^3	4.80×10^3
75 percentile	1.05×10^6	371.14	3.27×10^4	3.26×10^4

Table S5 Median concentrations of NH₃, C2 amines and C3 amines from 10th December 2018 to 6th January 2019.

Species	Unit	Night	Polluted Night	Clean-2 Night
		(20:00-04:00)	(Vis < 12 km)	(Vis ≥ 16km, [O ₃] ≥ 2×10 ¹¹ cm ⁻³)
NH ₃	Mixing ratio in ppb	2.8	3.3	1.9
	Concentration in cm ⁻³	7.6×10 ¹⁰	8.9×10 ¹⁰	5.1×10 ¹⁰
C2 Amines	Mixing ratio in ppt	2.4	2.6	1.6
	Concentration in cm ⁻³	6.3×10 ⁷	7.0×10 ⁷	4.4×10 ⁷
C3 Amines	Mixing ratio in ppt	1.2	1.4	0.74
	Concentration in cm ⁻³	3.1×10 ⁷	3.9×10 ⁷	2.0×10 ⁷

References

Jayne, J. T., Pöschl, U., Chen, Y.-m., Dai, D., Molina, L. T., Worsnop, D. R., Kolb, C. E., and Molina, M. J.: Pressure and Temperature Dependence of the Gas-Phase Reaction of SO₃ with H₂O and the Heterogeneous Reaction of SO₃ with H₂O/H₂SO₄ Surfaces, *The Journal of Physical Chemistry A*, 101, 10000-10011, 10.1021/jp972549z, 1997.